

Experimental evidence for Sm- C_G \rightarrow Sm- CP polymorphism in fluorinated bent-shaped mesogens

A. Eremin, S. Diele, G. Pelzl, H. Nádasi, and W. Weissflog

Institut für Physikalische Chemie, Martin-Luther-Universität Halle-Wittenberg, Mühlpforte 1, D-06108 Halle (Saale), Germany

(Received 27 June 2002; published 26 February 2003)

We report the experimental results on pure fluorinated bent-shaped mesogens showing very unusual textures and electro-optical behavior. In the view of recent publications such behavior can be explained by triclinic symmetry of the mesophase (Sm- C_G) formed by these compounds. Based on the results of the x-ray diffraction and electro-optical investigations, we give evidence for the Sm- $C_G \rightarrow$ Sm- CP polymorphism.

DOI: 10.1103/PhysRevE.67.021702

PACS number(s): 61.30.Eb, 64.70.Md, 77.84.Nh

I. INTRODUCTION

Almost 25 years ago a simple smectic phase with triclinic symmetry was proposed by de Gennes [1] and was called Sm- C_G phase (where G stands for general). However, experimental attempts to find such a phase among calamitic compounds did not succeed until recently. The discovery of the liquid crystalline mesophases formed by bent-shaped molecules promoted further research on the way to the Sm- C_G phase. Theoretical evidence for triclinic symmetry of a smectic phase with bent-shaped molecules can be found in the work by Brand *et al.* [2]. The tilt (clinic) θ of the molecular plane defined by the shape of the molecule results in the Sm- CP phase with C_2 symmetry (Fig. 1). Additionally, leaning of the molecules in the tilt plane leads to C_1 symmetry of the Sm- C_G phase. Pleiner *et al.* [3] suggested that the experimentally observed B_7 phase is identical to the Sm- C_G phase. Regarding experimental realization, an attempt to find triclinic symmetry in asymmetric bent-shaped molecules did not give any conclusive results [4]. At the same time, recent evidence of C_1 symmetry in free-standing films was reported by Chattham *et al.* [5].

Among the “banana phase” candidates for the mesophases with C_1 symmetry the B_7 phase has attracted particular interest because of the formation of exotic optical textures as well as the growth of serpentinelike germs and beaded filaments. Such behavior of optical textures clearly indicates a helical superstructure [6–8] of the B_7 phase. It can be assumed that the chirality of the phase [9] is responsible for the formation of macroscopic helical domains. The structure of this mesophase has not been understood up to now. X-ray investigations exclude a simple layer structure and point to a two- or three-dimensional superstructure. Although it should be emphasized that the lateral arrangement of the molecules is liquidlike in the B_7 phase.

There are also “banana phases” with the structural characteristics of the Sm- CP phase (simple layer structure, tilt of the molecules, polar order) which form screwlike nuclei on cooling of the isotropic liquid quite similar to the B_7 phase [10,11]. Nevertheless, because of a different structure this phase should not be designated as B_7 phase; it is another mesophase. A completely different type of chiral domains was observed by Thisayuktu *et al.* [12,13] in the high-temperature phase of a bent-shaped mesogen with naphthalene as central core. These domains of opposite handedness

grow as fractal nuclei and show distinct circular dichroism. For instance, such domains have also been generated by exposure to a triangular-wave field in a sulfur-containing bent-core mesogen [14].

Of particular interest was a bent-shaped compound with lateral fluorine substituents which was first described by Heppke *et al.* [11]. The mesophase of this compound which possesses a Sm- CP -like structure and exhibits a B_7 -like texture was the subject of detailed investigation done by Jákli *et al.* [15]. On the basis of electro-optical measurements a smectic phase with triclinic symmetry (Sm- C_G) was suggested.

In order to get a deeper insight into the nature of this phase we investigated shorter and longer homologues of this compound. Employing x-ray and electro-optical techniques we found a phase sequence I –Sm- X –Sm- CP – B_4 for all members of the series. From the experimental findings plausible arguments can be derived that the high-temperature phase Sm- X is a smectic phase with C_1 symmetry.¹ Furthermore, this high-temperature phase is able to form screwlike and telephone-wire-like nuclei as well as large chiral domains depending on the experimental conditions. It is re-

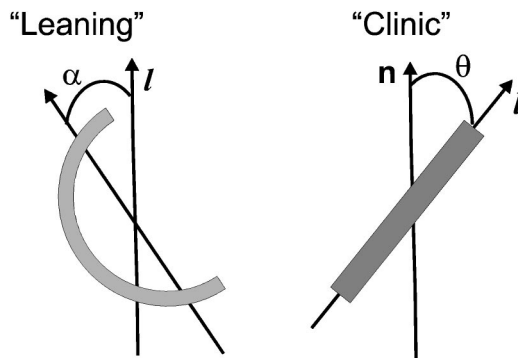


FIG. 1. Orientation of a bent-shaped molecule in the Sm- C_G phase. The molecular plane is tilted by tilt angle θ (“clinic”). The molecular long axis is inclined in the tilt plane by the “leaning” angle α .

¹According to a private communication [28], the high-temperature Sm- X phase discussed in this paper possesses a modulated layer structure with an unusual long period in the direction perpendicular to the layer normal.

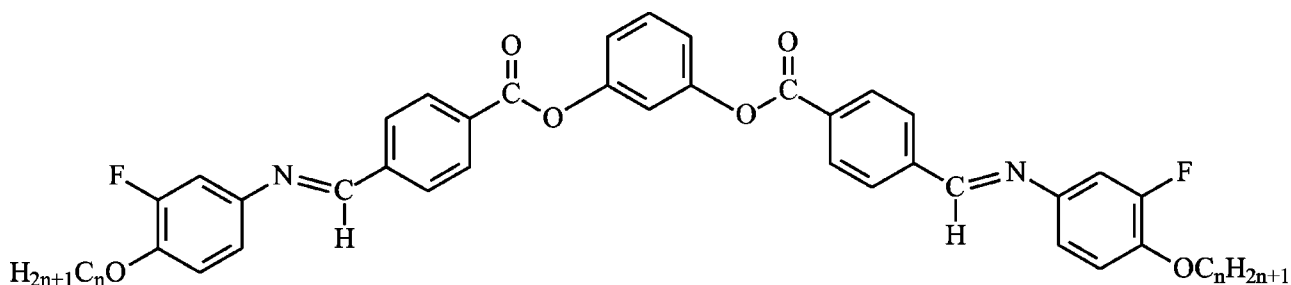


FIG. 2. Molecular structure of compounds 8–12.

markable that the large chiral domains remain unchanged at the transition into the B_4 phase.

II. EXPERIMENT

The compounds under investigation are 1, 3-phenylene bis[4-(4- n -alkoxy-3-fluoro-phenylimino-methyl)benzoates] $n = 8, \dots, 12$ (Fig. 2). The phase transition temperatures (Table I) were determined with a Perkin-Elmer differential scanning calorimeter (DSC Pyris 1) at a rate of 5 K/min. Optical studies were made using a polarizing microscope equipped with a Linkam THMS-600 temperature controlled heating stage. X-ray investigations on nonoriented samples were performed using a Guinier film camera or a Guinier goniometer; x-ray investigations on oriented samples were carried out with a two-dimensional detector (HI-Star, Siemens AG). Electro-optical measurements were made using an experimental setup described in the earlier paper [16]. The switching current was measured using the triangular wave voltage method.

III. RESULTS

A. X-ray diffraction measurements

1. Powder samples

X-ray diffraction (XRD) measurements have been performed using film Guinier technique. The patterns of the Sm- X possess two commensurable small-angle reflections and one diffuse scattering maximum in the wide-angle region ($\sim 10^\circ$), which points to a layered structure with liquidlike order within the layers. No incommensurable reflections have been observed indicating that the structure of the Sm- X phase is different from the structure of the B_7 phase de-

TABLE I. Phase behavior and transition temperatures.

Compound	n	Cr	B_4^a	Sm- CP	Sm- X	I
8 [10]	8	●	129 (● 98)	●	164	● 166 ●
9	9	●	123 (● 101)	●	153	● 163 ●
10 [11,15]	10	●	124 (● 99)	●	147	● 163 ●
11	11	●	121	●	141	● 162 ●
12	12	●	120 (● 98)	●	132	● 160 ●

^aThe B_4 phase can be supercooled up to room temperature, the inverse transition $B_4 \rightarrow$ Sm- CP takes place about 10–12 °C above this temperature.

scribed in Ref. [6]. The layer spacing is temperature independent, neither does it change during the Sm- $CP \rightarrow$ Sm- X transition nor at the transition into the B_4 phase.

In Table II the layer spacing d and the effective molecular lengths L are given. A bending angle of 120° based on our previous experimental observations [17,18] is assumed in the estimation of the effective molecular length.

The dependence of the layer spacing on the length of the terminal chain exhibits a linear trend. The layer spacing is clearly smaller than the effective molecular length which can be brought about by a tilted arrangement of the molecules within the smectic layers. From the ratio d/L the tilt angle of $\sim 32^\circ$ has been estimated.

Measurements of the correlation lengths from the full width at half maximum give us some more information on the difference between the Sm- X , Sm- CP , and B_4 phases (Fig. 3). In the high-temperature Sm- X phase of the compound 12 the correlation length ($\xi = 900 \text{ \AA}$) is nearly temperature independent. The transition into the Sm- CP phase is accompanied with a continuous increase of the correlation length. The small-angle reflection becomes considerably broad in the B_4 phase, resulting in abrupt decrease of the correlation length till 600 \AA (Fig. 3). It is in agreement with the earlier described results [17] where a line broadening was observed for the wide- and small-angle reflections on cooling the sample from the crystalline B_3 into the B_4 phase.

2. Oriented samples

A characteristic feature of the patterns obtained from surface-oriented samples on the Sm- X phase, is the occurrence of four reflections in the small-angle region [Figs. 4(a) and 4(b)]. The pairs of reflections—along the equator and the meridian—have quite different mosaicities and, therefore, cannot correspond to one common lattice. Additionally, they reflect the same periodicity that has also been proved by the

TABLE II. Results of the x-ray measurements.

Compound	Molecular length $L(\text{\AA})$	Spacing $d \pm 0.5 (\text{\AA})$	Tilt angle (deg)
8	45.3	38.5	31.3
9	47.5	40.5	31.4
10	49.5	41.8	32.5
11	51.6	43.5	32.6
12	54.4	45.5	33.2

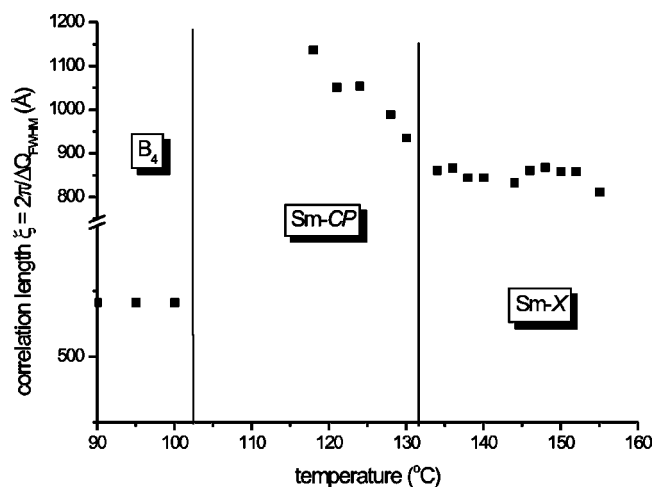


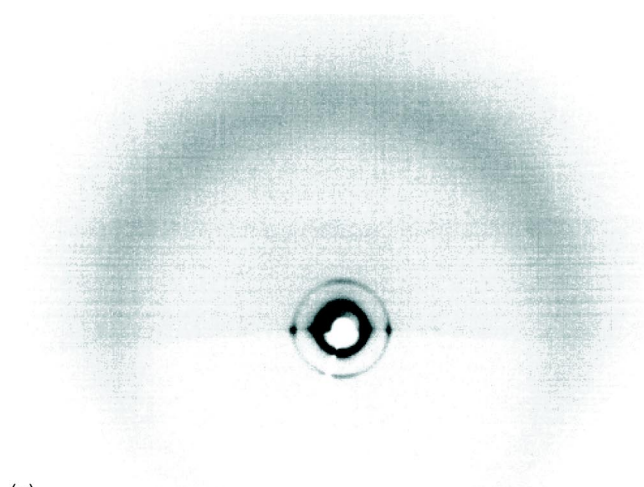
FIG. 3. Temperature dependence of the longitudinal correlation length ξ .

Guinier method on powderlike samples. Thus, it is obvious that these reflections originate from differently oriented domains where the smectic layers are parallel and perpendicular to the substrate surface. When the terminal chains are short (compound 8) the smectic layers prefer laying parallel to the substrate. The longer chained homologues prefer orienting perpendicular to the substrate surface (compound 12). For compound 9 the probability is equal for growing in both directions.

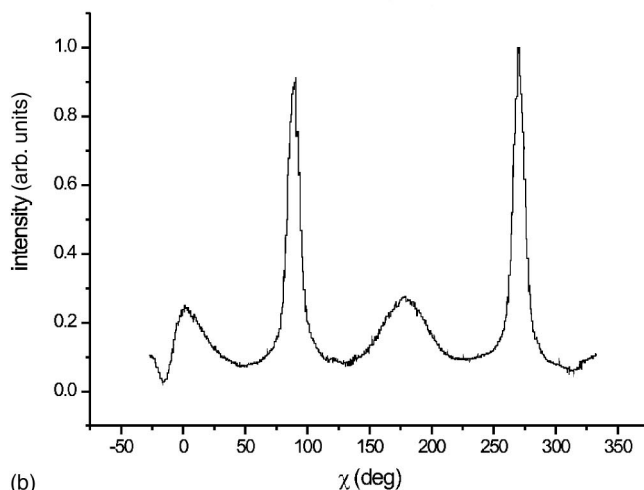
In the wide-angle region there is a broad diffuse halo showing the absence of positional order within the smectic layers. At first sight the diffuse halo is uniformly distributed over a circle. Normalization technique described in Ref. [16] enables us to extract the structure of the diffuse scattering distribution. Two distinct maxima in a wide-angle region have been found [Fig. 4(c)], which stands for the tilt of the molecules with respect to the layer normal. The tilt angle of $\sim 33^\circ$ found from the diffuse scattering measurement is in good agreement with the value obtained from the analysis of the layer spacing. The orientation completely disappears after the transition into the B_4 phase. Finally, the results of the x-ray experiments suggest that the Sm-X phase is a smectic phase without in-plane order formed by tilted molecules. To differentiate between the properties of the Sm-X and the Sm-CP phases we performed electro-optical measurements.

B. Electro-optical investigations and texture observations

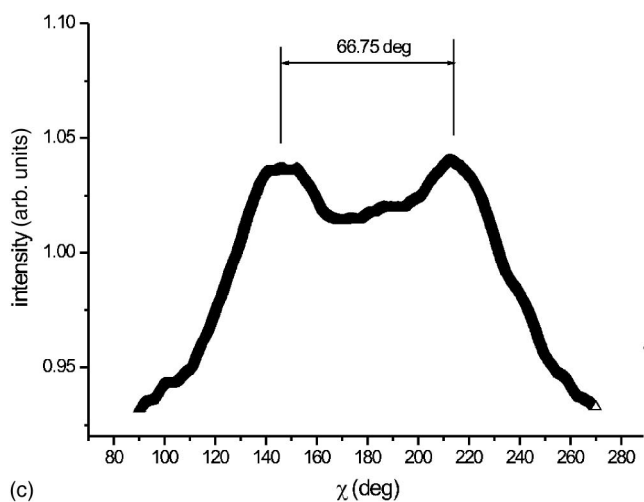
The electro-optical measurements have been made using $10\text{-}\mu\text{m}$ indium tin oxide (ITO) cells (EHC Corp.) and triangular wave technique. On rapid cooling the sample from the isotropic phase a grainy nonspecific texture appears. When the cooling rate is slow (0.1 K/min) different kinds of growing domains are observed: colored and gray ribbonlike domains as well as screwlike and telephone-wire filaments (Fig. 5). When the texture is not completely formed and the growing domains are surrounded by the isotropic liquid, application of an electric field can affect the microscopic texture. Depending on the polarity of the field, the gray ribbons grow or shrink. Exposure of the ribbons to an electric field



(a)



(b)



(c)

FIG. 4. (a) X-ray pattern of the surface oriented sample; (b) χ scan of the layer reflections showing four maxima: along and perpendicular to the equator of the pattern; (c) extracted intensity distribution of the wide-angle diffuse scattering.

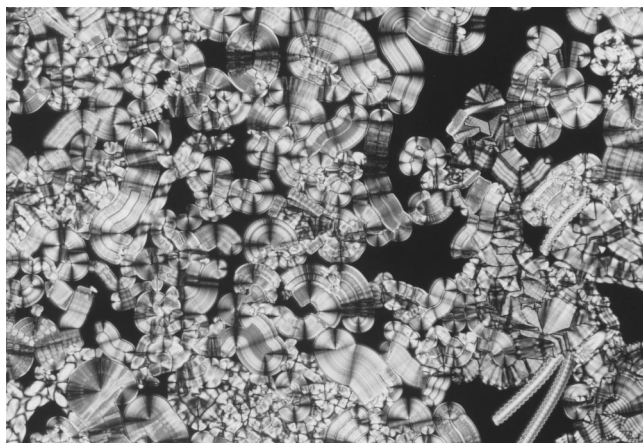
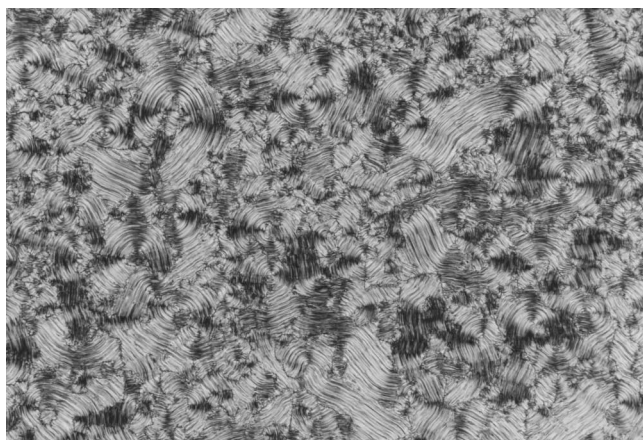


FIG. 5. Formation of the Sm-X phase on slow cooling of the isotropic liquid (compound 9, $T=156^\circ\text{C}$) (size $250\times 375\ \mu\text{m}$).

results in coiling of the gray ribbons into spirals. Depending on the polarity of the external field the spirals are formed clock or counterclockwise (shrinking of a ribbon leads to growing and coiling of another end of the ribbon). This effect



(a)



(b)

FIG. 6. Microscopic texture of the Sm-CP phase of the compound 10 at $T=133^\circ\text{C}$: (a) $E=0$, (b) $E=\pm 20\ \text{V}/\mu\text{m}$ (size $250\times 375\ \mu\text{m}$).

is thresholdless, even weak fields can promote growing or shrinking of the domains. This finding shows that the ribbons are polar and the polarization vector has a component parallel to the substrate surface. Application of an electric field produces a torque $\mathbf{M}=\mathbf{p}\times\mathbf{E}$ of the gray ribbonlike domains. The direction of the momentum depends on the orientation of the electric field and makes the ribbons twist into spirals: right or left handed, depending on the direction of the field. These observations are consistent with those given by Jákli *et al.* [15] in favor of the Sm- C_G phase.

In contrast, the screwlike domains have quite different behavior. Coiling of filaments is another way to compensate the polarization to satisfy $\nabla\cdot\mathbf{p}=0$. Fields above a threshold lead to an abrupt change of the sign of the gradient angle of the helix. Long exposure to an electric field eventually destroys screwlike domains and promotes growing of the flat nuclei.

As soon as the texture covers the whole view field of the microscope the application of the electric field does not markedly affect the texture. The microscopic texture exhibits four kinds of flat domains with different birefringence (similar to Refs. [7,15]): gray, green, red, and yellow. In high fields ($\sim 20\ \text{V}/\mu\text{m}$) small stripes appear and the extinction crosses of the green domains experience very small turns, but no current response could be detected. Other domains just slightly change birefringence. A longer exposure to the strong electric field results in transformation of different domains into the red fanlike domains that are insensitive to the external field.

On further cooling, a phase transition takes place which can be easily seen by a change of the optical texture from fanlike into a grainy texture [Fig. 6(a)]. In addition, the electro-optical response is completely different. In this low-temperature phase the switching occurs at a moderately low threshold ($\sim 2.5\ \text{V}/\mu\text{m}$); the field-induced texture change is independent of the polarity of the field [Fig. 6(b)]. The repolarization current response exhibits two peaks per half period of the applied triangular voltage indicating an antiferroelectric (AFE) ground state. After the phase transition, the switching polarization reaches its saturated value fast and

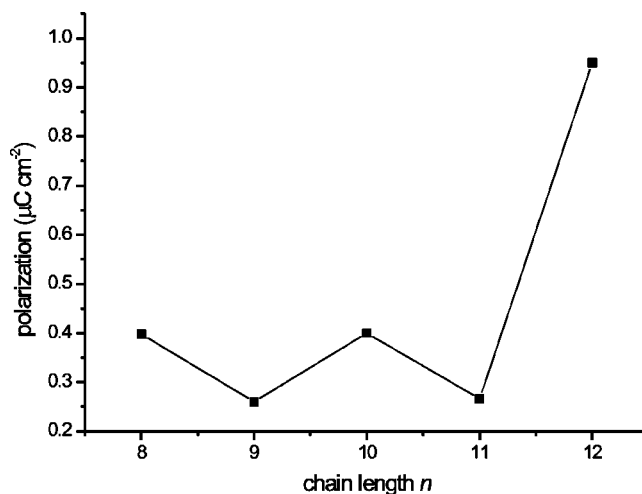


FIG. 7. Odd-even effect of the dependence of the spontaneous polarization on the length of the terminal chains.

remains nearly independent of the temperature. This behavior is typical for the Sm-CP phase. Surprisingly, the values of the spontaneous polarization show pronounced odd-even effect even despite that the terminal chains are quite long (Fig. 7). The transition between the high-temperature phase, preliminary designated as Sm-X , and the Sm-CP ($\text{Sm-C}_S P_A$) phase was found for all homologues studied, but as seen from Table I the temperature of this transition increases with decrease of the terminal chain length. It should be noted that this transition could not be detected by calorimetry and x-ray measurements.

It is remarkable that an application of a strong electric field may induce a transition from the Sm-X into the Sm-CP phase. Above a threshold that depends on the temperature a clear texture change is observed that is accompanied by current response characteristic for an antiferroelectric behavior. As an example in Fig. 8(a) a field dependence of the current response in the Sm-CP phase is shown. Below a threshold E_{th1} for $\text{AFE} \rightarrow \text{FE}$ transition there is no repolarization peak. As soon as the amplitude of the external field reaches the switching threshold a current peak centered in the maximum of the external field (top of the “triangular”) arises. In contrast, above the $\text{Sm-CP} \rightarrow \text{Sm-X}$ transition there is no current response above the threshold and the optical texture looks intact. However, when the amplitude of the external voltage is higher than a threshold E_{th} ($E_{th1} < E_{th}$) the switching suddenly appears [Fig. 8(b)]. Moreover, the maximum of the current response peak is not in the maximum of the external field anymore: the threshold for $\text{AFE} \rightarrow \text{FE}$ remains as in the Sm-CP phase ($\sim 2.5 \text{ V}/\mu\text{m}$). Such effect can be caused by a field induced phase transition from the Sm-CP into the Sm-X phase governed by the temperature dependent threshold E_{th} . The diagram in Fig. 8(c) shows the temperature dependence of the threshold E_{th} for the $\text{Sm-CP} \rightarrow \text{Sm-X}$ transition as well as the thresholds for $\text{AFE} \rightarrow \text{FE}$ transitions (E_{th1} and E_{th2}). It should be noted that the phase transition $\text{Sm-X} \rightarrow \text{Sm-CP}$ (as well as the field-induced phase transition) has also been reported for compound 10 in Ref. [26].

As was shown before, on very slow cooling the isotropic liquid screwlike domains and beaded filaments of the Sm-X phase appear indicating a helical superstructure like in the B_7 phases. In the compounds under discussion another kind of chiral domains can occur at certain cooling rates. These domains grow as fractal nuclei and coalesce into large areas with opposite optical rotation. When one of the polarizers is turned away from the crossed position clockwise by a small angle ($2\text{--}10^\circ$), dark (blue) and light (yellow) domains become visible. Rotating the analyzer anticlockwise by the same angle the effect is reversed; that means, the previously dark domains now appear light and vice versa (Fig. 9). These chiral domains rotate the polarized light clockwise or anticlockwise, respectively. The domains can be also distinguished by illuminating the sample with left or right circular polarized light in the reflection mode of the microscope. Depending on the sign of the circular polarized light bright and dark domains could be observed. It should be noted that the chiral domains do not affect the color or the light transmission if the sample is rotated. This is a clear indication that the axis of the helical structure is perpendicular to the substrate

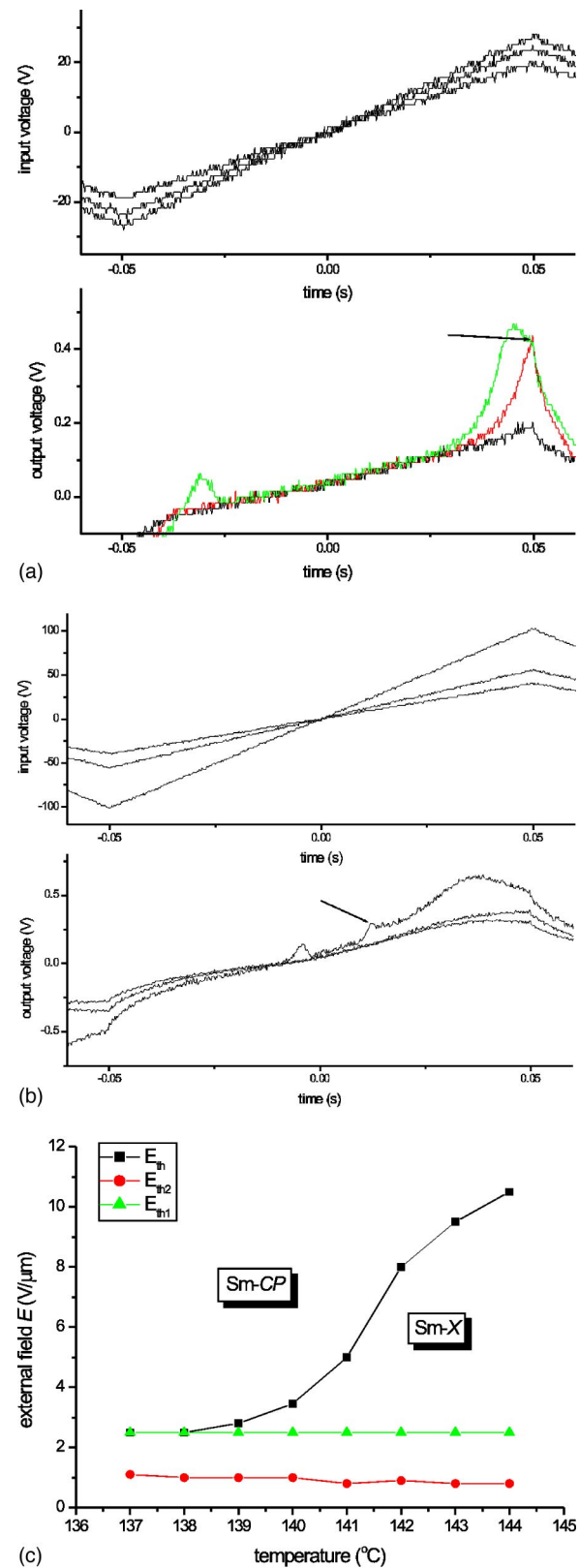
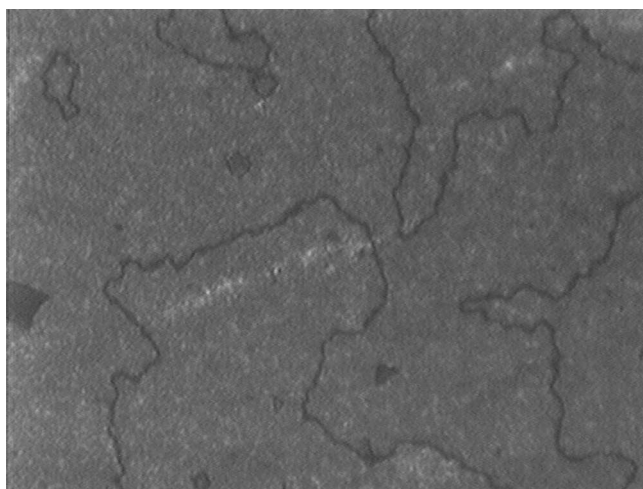
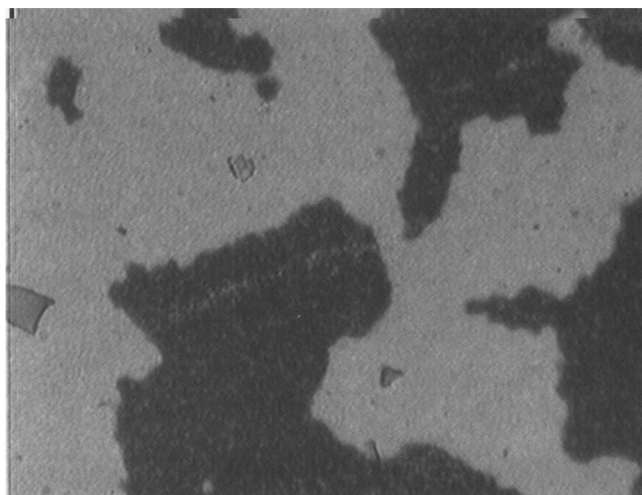


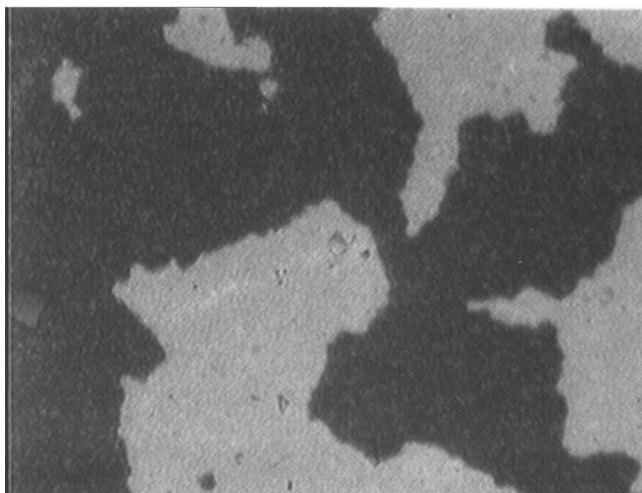
FIG. 8. Field-induced $\text{Sm-X} \rightarrow \text{Sm-CP}$ transition: external field and current response in (a) the Sm-CP phase and (b) in the Sm-X (appearance of the repolarization current is marked by an arrow), (c) temperature dependence of the thresholds E_{th} ($\text{Sm-X} \rightarrow \text{Sm-CP}$), E_{th1} ($\text{AFE} \rightarrow \text{FE}$), E_{th2} ($\text{FE} \rightarrow \text{AFE}$).



(a)



(b)



(c)

FIG. 9. Microscopic texture of the Sm-CP phase of compound 8 at (a) crossed polarizers; (b) and (c) rotation of one polarizer by $+2^\circ$ and -2° , respectively, from the crossed position (130°C) (size $200\times 250\ \mu\text{m}$).

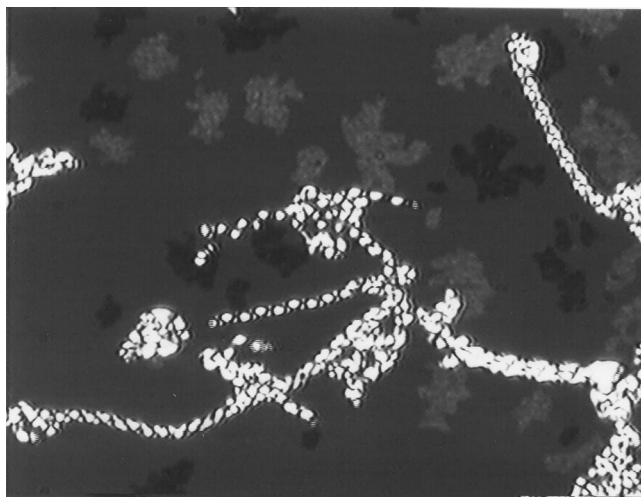


FIG. 10. Coexistence of the screwlike and chiral fractal domains in the Sm-X phase of compound 9. One polarizer deviates by 5° from the crossed position (size $200\times 250\ \mu\text{m}$).

planes. Such chiral domains were first described by Thisayukta *et al.* [12,13]. We found that the tendency to form such domains is different for the homologous compounds and if the glass substrates are treated with a surfactant solution the formation of these domains is promoted; sometimes nearly the whole preparation adopts such texture.

On cooling the Sm-X phase the chiral domains remain unchanged at the transition into the Sm-CP and B_4 phases. In the B_4 phase the texture shows nearly extinction between the crossed polarizers and the contrast between the domains of opposite handedness is less pronounced. These domains neither change upon a reversed transition on heating from the B_4 phase. Only the formation of the Sm-CP phase from the B_4 phase is delayed, taking place at about 10°C higher temperature. Similar behavior has also been found in other compounds with a phase sequence B_4 - B_2 [19]. It should be noted that by adding of a chiral dopant the ratio of domains with a different handedness can be clearly changed.

Depending on the experimental conditions (cooling rate; surface treatment) we observed an interesting behavior. During the nucleation of the Sm-X phase, one-dimensionally growing screwlike domains as well as large chiral domains grow simultaneously (Fig. 10). The screwlike domains further transform into a grainy texture, whereas the large chiral domains remain unchanged.

It seems that the screwlike domains and the chiral ones have the same origin—the chirality of the smectic layers. Obviously, the nucleation energies of both types of chiral domains are not much different so that they can coexist under certain conditions.

IV. DISCUSSION

Based on our XRD measurements we can conclude that the high-temperature Sm-X phase is a tilted smectic phase without in-plane order like a Sm-C phase. It excludes two- or three-dimensional structures of the original B_7 phase [6–8,18,20,21]. Our results are in agreement with the results

published by Jákli *et al.* [15] which were obtained from the investigation of compound 10. Really, the ribbonlike filaments are polar and the extinction crosses are oriented parallel to the analyzer and the polarizer. At the same time, an assumption of a ferroelectric antclinic structure ($\text{Sm-}C_A P_F$) is not satisfactory. The $\text{Sm-}C_A P_F$ phase has been found only in chiral bent-shaped molecules and it can be switched within milliseconds, while the $\text{Sm-}X$ phase lacks the electro-optical response.

On the other hand, the growth of the helical filaments indicates essentially chiral structure of the phase. As shown by Jákli *et al.* [7] screwlike domains are built up by smectic filaments. The growth of the smectic filaments takes place via the absorption of the molecules from the surrounding isotropic phase by the outermost layers. The molecules in inner layers have to be pushed by the absorbed molecules. It results in an increasing compression force and leads to an undulation instability [7]. The difference between nonhelical and helical filaments becomes apparent only when modulation appears. Nonhelical filaments take a serpentine-like form, whereas helical domains form coils. Two kinds of helical filaments (screwlike and telephone-wirelike) have quite different behavior. Experimentally we observed that the bright, tight screw filaments grow under slow cooling. In contrast, the thin telephone-wire filaments appear at fast cooling and their growth is accompanied with bending. Slow cooling allows minimizing the surface free energy in the isotropic-liquid crystal interface by forming the coils. On fast cooling, there is no time to minimize the surface energy and thin bent filaments appear. The twist deformation caused by chirality of the phase is replaced by formation of the coils since a helical shape has less elastic energy than the corresponding twisted form [7].

The behavior of the ribbon filaments in the electric field suggests a nonzero polarization component perpendicular to the smectic layers. This finding excludes the $\text{Sm-}CP$ structure with C_2 symmetry for the high-temperature $\text{Sm-}X$ phase. At the same time if the molecules in addition to the antclinic arrangement experience leaning in the tilt plane, the out-of-plane polarization is allowed. It corresponds to the lowest C_1 symmetry [15] which is possessed by the general $\text{Sm-}C_G$ phase considered by de Gennes [1]. Jákli *et al.* [15] concluded from the experimental findings that the leaning angle α decreases with decreasing temperature so that, in principle, a transition $\text{Sm-}C_G \rightarrow \text{Sm-}CP$ seems to be possible. Our experiments have shown that such transition does exist in the homologues. The high-temperature $\text{Sm-}X$ ($\text{Sm-}C_G$) phase is not switchable, which can be due to the

stronger sterical hindrance that does not let the leaning molecules turn in the smectic plane compared with nonleaning molecules in the $\text{Sm-}CP$ phase. A continuous decreasing of the leaning angle α with decreasing temperature may result in the second or weakly first order transition into the switchable $\text{Sm-}CP$ phase [15], which is in agreement with the theoretical predictions [22,27]. In our experiments no signal on the DSC curve was observed indicating the second order $\text{Sm-}C_G \rightarrow \text{Sm-}CP$ transition. This interpretation is also in a good agreement with the observed field induced transition into the $\text{Sm-}C_G$ phase. A few degrees above the transition temperature an electric field can decrease the leaning angle α , resulting in the switchable structure with C_2 symmetry of the $\text{Sm-}CP$ phase. One of the possibilities for decreasing in the molecular tilt has been proposed in the Ref. [23] by a so-called electrodisclination effect. An external electric field reduces the mean square fluctuations $\langle u^2(E) \rangle$ of the smectic layer spacing leaving the d values constant, which results in the decrease of the tilt. In case of the $\text{Sm-}C_G$ phase the molecular tilt can be separated in two components “clinic” angle θ and “leaning” α . Leaning of the bent molecules creates large difference in free volume within the smectic layer which makes leaning of the molecules sterically “unfavorable.” Therefore, it seems plausible that the leaning angle α should decrease faster than θ leading to the transition into the $\text{Sm-}CP$ phase with $\alpha=0$ and $\theta \neq 0$.

The arrangement of the molecules in chiral domains of the B_4 phase [24,25] is not yet clear. Our optical studies show that the light transmission of these domains does not change on rotating the sample. On the other hand, these experimental findings point to a helical arrangement of the molecules like in a $\text{Sm-}C^*$ phase where the helix axis is perpendicular to the substrate plane. This assumption is also confirmed by the observation that in thin samples of the B_4 phase these chiral domains show nearly extinction between crossed polarizers. In this case the smectic layers are parallel to the substrate planes. The results of our optical studies are also compatible with an arrangement of the smectic layers perpendicular to the substrates as in the twist grain boundary (TGB) phase.

ACKNOWLEDGMENTS

The author would like to express his sincere appreciation to H. Brand and B. I. Ostrovskij for very useful discussions. This work was supported by the Deutsche Forschungsgemeinschaft (DFG) and the Fonds der Chemischen Industrie.

-
- [1] P.G. de Gennes, *Physics of Liquid Crystals* (Clarendon Press, Oxford, 1975).
 [2] H.R. Brand, P.E. Cladis, and H. Pleiner, *Eur. Phys. J. B* **6**, 347 (1998).
 [3] H. Pleiner, H.R. Brand, and P.E. Cladis, *Ferroelectrics* **243**, 291 (2000).
 [4] A. Jákli, Ch. Lischka, W. Weissflog, G. Pelzl, and A. Saupe,

- Liq. Cryst.* **27**, 715 (2000).
 [5] N. Chattham, E. Körblova, R. Shao, D.M. Walba, J.E. Macmillan, and N.A. Clark (unpublished).
 [6] G. Pelzl, S. Diele, A. Jákli, Ch. Lischka, I. Wirth, and W. Weissflog, *Liq. Cryst.* **26**, 135 (1999).
 [7] A. Jákli, Ch. Lischka, W. Weissflog, G. Pelzl, and A. Saupe, *Liq. Cryst.* **27**, 1405 (2000).

- [8] D.M. Walba, E. Körblova, R. Shao, J.E. MacLennan, D.R. Link, M.A. Glaser, and N.A. Clark, *Science* **288**, 2181 (2000).
- [9] D.R. Link, G. Natale, R. Shao, J.E. MacLennan, N.A. Clark, E. Körblova, and D.M. Walba, *Science* **278**, 1924 (1997).
- [10] C.K. Lee and L.C. Chien, *Ferroelectrics* **243**, 231 (2000).
- [11] G. Heppke, D.D. Parghi, and H. Sawade, *Ferroelectrics* **243**, 269 (2000).
- [12] J. Thisayukta, H. Kamee, S. Kawauchi, and J. Watanabe, *Liq. Cryst.* **346**, 63 (2000).
- [13] J. Thisayukta, Y. Nakayama, S. Kawauchi, H. Takezoe, and J. Watanabe, *J. Am. Chem. Soc.* **122**, 7441 (2001).
- [14] G. Heppke, D.M. Parghi, and H. Sawade, *Liq. Cryst.* **27**, 313 (2000).
- [15] A. Jákli, D. Krüerke, H. Sawade, and G. Heppke, *Phys. Rev. Lett.* **86**, 5715 (2001).
- [16] A. Eremin, S. Diele, G. Pelzl, H. Nádasi, W. Weissflog, J. Salfetnikova, and H. Kresse, *Phys. Rev. E* **64**, 051707 (2001).
- [17] G. Pelzl, S. Diele, and W. Weissflog, *Adv. Mater.* **11**, 707 (1999).
- [18] W. Weissflog, H. Nádasi, U. Dunemann, G. Pelzl, S. Diele, A. Eremin, and H. Kresse, *J. Mater. Chem.* **11**, 2748 (2001).
- [19] H. Nádasi, Ch. Lischka, W. Weissflog, I. Wirth, S. Diele, G. Pelzl, and H. Kresse, *Mol. Cryst. Liq. Cryst.* (to be published).
- [20] J.P. Bedel, J.C. Rouillon, J.P. Marcerou, M. Laguerre, H.T. Nguyen, and M.F. Achard, *Liq. Cryst.* **27**, 1411 (2000).
- [21] D.S. Shankar Rao, Geetha G. Nair, S. Krishna Prasad, S. Anita Nagamani, and C.V. Yelamaggad, *Liq. Cryst.* **28**, 1239 (2001).
- [22] H. Pleiner, H.R. Brand, and P.E. Cladis, *Ferroelectrics* **248**, 291 (2000).
- [23] A. Jákli, G.G. Nair, C.K. Lee, and L.C. Chien, *Liq. Cryst.* **28**, 489 (2000).
- [24] T. Sekine, T. Niori, M. Sone, J. Watanabe, S.W. Choi, Y. Takanishi, and H. Takezoe, *J. Jpn. Appl. Phys.* **36**, 6455 (1997).
- [25] G. Heppke, D. Krüerke, C. Löning, D. Löttsch, S. Rauch, and N-K. Sharma (unpublished).
- [26] A. Jákli, G.G. Nair, H. Sawade, and G. Heppke, *Liq. Cryst.* (to be published).
- [27] A. Jákli and P. Tolédano, *Phys. Rev. Lett.* **89**, 275504 (2002).
- [28] N.A. Clark (private communication).